JOURNAL OF INFORMATION AND COMMUNICATION TECHNOLOGY
https://e-journal.uum.edu.my/index.php/jict

How to cite this article:
Siddique, M. T., Venkat, I., & Shah Newaz, S. H., Tajuddin, S. (2025). Robust single sample per person face recognition with probabilistic illumination enhancement. *Journal of Information and Communication Technology, 24*(3), 90-112. https://doi.org/10.32890/jict2025.24.3.5

Robust Single Sample Per Person Face Recognition with Probabilistic Illumination Enhancement

[1]Muhammad Tariq Siddique, [2]Ibrahim Venkat, [3]Shah Hasan Shah Newaz & [4]Sharul Tajuddin
[1,2,3&4]School of Computing and Informatics, Universiti Teknologi Brunei, Brunei Darussalam
[2]School of Computer Sciences, Universiti Sains Malaysia, Malaysia
[1]Department of Computer Science, Bahria University, Pakistan

[*1]tariqsiddique.bukc@bahria.edu.pk
[2]ibrahim.venkat@utb.edu.bn
[3]shah.newaz@utb.edu.bn
[4]sharul.tajuddin@utb.edu.bn
*Corresponding author

Received: 5/5/2025 Revised: 26/6/2025 Accepted: 5/7/2025 Published: 31/7/2025

ABSTRACT

The challenges imposed by the Single Sample Per Person face recognition problem become especially critical when face images are captured in uncontrolled environments, which typically involve variations in illumination, facial expression, pose, occlusion, and more. In particular, illumination changes caused by poor lighting conditions can significantly degrade the performance of face recognition systems. In this paper, we investigate the SSPP face recognition problem in the presence of potential illumination variation and propose a two-fold approach. Firstly, we analyse and quantify the illumination variations in face images and then normalise these variations based on a probabilistic image enhancement approach. Subsequently, the feature embedding process was performed using the deep learning-based FaceNet system, and finally, faces were classified using the classical Support Vector Machine. The performance of the proposed approach is demonstrated through comprehensive experiments compared to state-of-the-art techniques. The proposed method achieved significant accuracy improvements, attaining 96.17% and 95.68% for 20 and 30 subjects, respectively, on the Extended Yale-B dataset. The performance of the proposed method is evaluated and exhibits superiority in handling illumination compared to state-of-the-art counterparts.

Keywords: Illumination, probabilistic image enhancement, Retinex theory, SSPP face recognition, FaceNet, SVM.

INTRODUCTION

Face recognition has been proven to be a prominent, cost-effective biometric that has potential applications in human identification and related surveillance systems. It is also considered non-obtrusive due to the ease in image acquisition (Azmeen & Borah, 2021). A face image can encode rich information, including facial expressions, gender, age, ethnic origin, identity, and more. However, these vast variations make face recognition a challenging problem in machine learning. For example, expressions are transient as compared to the ageing factor and affect face recognition considerably with variations such as head pose, illumination, occlusion, and low resolution (Arigbabu et al., 2015; Huang & Alhlffee, 2023; Oloyede et al., 2020; Tran et al., 2022). When a single image is enrolled (gallery image) for training purposes, it is referred to as the classical Single Sample Per Person (SSPP) problem. The goal is to recognise and identify probe images subject to vast variations, as fewer training samples are available. SSPP poses a significant challenge to computer vision researchers (Liu et al., 2015). Despite the challenges, the SSPP-based face recognition (SSPP FR) has many practical applications in the real world, including access control, law enforcement, criminal identification, video surveillance, and person re-identification (Mokhayeri et al., 2018; Ye et al., 2019).

It has been observed that when the environment is controlled, SSPP FR systems perform well with outstanding accuracy. However, in an uncontrolled environment, recognition accuracy decreases considerably and fails to provide reasonable performance for person identification. Real-world applications require significantly better performance. Various studies have been reported in the literature to address the problem of SSPP using different Machine Learning techniques, despite variations such as pose, expression, occlusion, and illumination conditions. For example, segmentation of images into small patches and calculating distance using the k-nearest neighbors (k-NN) algorithm (Zhang et al., 2021), decompositions of face images into three channels based on the different features, i.e., local, global, and textual classification using the k-NN algorithm (Adjabi et al., 2021), and reconstruction of images using a variation model and augmented dictionary (Mokhayeri & Granger, 2020) are a few techniques that managed to address this SSPP successfully.

Despite illumination variation being a potential issue in surveillance applications, fewer investigations have been proposed to address the problem of image degradation caused by lighting conditions. In this paper, we address the SSPP FR with an emphasis on illumination variations by complementing the Probabilistic Image Enhancement method (PIE) (Fu et al., 2015) with deep learning. We believe that the PIE-based Illumination Correction for SSPP with deep learning features (PICS-DL) is a novel approach. We perceive that the PIE-based Illumination Correction with deep learning features, proposed in this paper and named PICS-DL, is quite novel.

RELATED WORK

Variations in illumination conditions affect the texture and luminosity of images, and also create shadowing effects that may alter facial appearance. These changes may cause problems in the process of person identification in a real-world environment, especially when having a single sample for face recognition. To address the SSPP FR problem under uncontrolled conditions, several efforts have been made in the past decade. Notably, the reported studies proposed different solutions for SSPP FR under uncontrolled conditions.

The primary issue with SSPP is the limited availability of a single image (gallery image) for training purposes, which creates limitations for deep learning (DL) models based on a Deep Neural Network (DNN). Despite this, several notable deep learning models have shown promise in addressing the performance of face recognition systems. Wang and Deng (2021) presented a survey on deep learning, describing Deep ID, FaceNet (Schroff et al., 2015) and DeepFace (Taigman et al., 2014) share insights on DL-based face recognition algorithms. A survey conducted by Mehdipour Ghazi and Kemal Ekenel (2016) discussed different existing studies based on face recognition with DL. However, they have also revealed that the performance of face recognition could improve with the use of appropriate pre-processing techniques.

Several studies have reported additional advancements in DL models. Abdelmaksoud et al. (2020) increase the number of images for training by proposing 3D face reconstruction. The authors have created a dictionary that includes pose variations. The Convolutional Neural Network (CNN) and AlexNet model were used for both training and testing the learning model. Yang et al. (2020) introduced a method to learn intra-class features. They have designed a dictionary-based learning approach that leverages local and global intra-class variations and learns deep features with the aid of CNN layers. A pre-trained model, DenseNet121, has been applied to the attendance system using CNN (Filippidou & Papakostas, 2020). The authors have used custom datasets to compare five pretrained models. Ríos-Sánchez et al. (2019) applied FaceNet and OpenFace models for mobile applications that operate in different environmental conditions. The authors have used these models for identification and verification problems with the SSPP constraint.

Moreover, generative adversarial networks and autoencoders have been utilised to address illumination constraints in various datasets (Zhang et al., 2019). Silva and Farias (2025) proposed Adversarial Disentangling Variational Autoencoder (AD-VAE), a novel framework that integrates Variational Autoencoders and Generative Adversarial Networks to address challenges such as illumination and occlusion in SSPP face recognition. Cuculo et al. (2019) used a data augmentation scheme to enhance the training sample size, whereas deep features are learned using a DNN. Later, a sparse sub-dictionary learning is created using linear discriminant analysis for the classification problem. It has been observed that no illumination effect is generated during the augmentation process. Zeng et al. (2018) proposed a technique for expanding the sample size to train the CNN. Then, the model was fine-tuned to enhance its recognition performance. However, it has been observed that the illumination effects generated by expanding the sample size have been insufficient for achieving a desirable recognition rate. Other studies (Ríos-Sánchez et al., 2019; Zeng et al., 2017; Zhang et al., 2019) have contributed valuable insights using generative and data expansion techniques to improve SSPP face recognition.

Some studies have focused on hybrid approaches that blend handcrafted and learned features. A Tree-structured Parzen Estimator-based Bayesian optimisation technique was proposed by Bouchene (2024) as a novel approach to optimise Histogram of Oriented Gradients (HOG) parameters and image size for facial recognition. Fei et al. (2024) presented a novel approach for learning multiple subspace features by applying singular value decomposition (SVD). Liu et al. (2021) proposed extracting middle-level semantic features for the SSPP problem using a Self-Organizing Map (SOM) and a Bag-of-Features (BoF) approach. They achieved good accuracy in their study; however, the utilisation of Scale Invariant Feature Transformation (SIFT) descriptors exceeded the computational time and cost for extracting the local features. Gan et al. (2020) created an auxiliary dictionary using virtual mirror images. Later, each probe image is represented by a patch using sparse representation.

The computational complexity of the problem for larger data sets can be increased by illumination compensation and normalisation, which play a crucial role in face recognition. Hence, this illumination variation has been considered a challenging task for the SSPP FR problem (Zeng et al., 2018). A survey was conducted on uneven illumination for images, in which the authors addressed different illumination models, background and shadow correction techniques, and methods for correcting uneven and non-uniform illumination (Dey, 2019).

A substantial body of research focuses on illumination compensation and image enhancement, both of which are crucial for improving performance in SSPP scenarios. In the literature, significant work has been reported on applying various image enhancement techniques to solve image classification problems. Another study reported the application of illumination normalisation for face recognition (Yi et al., 2015). The approach initially subdivided the face images into local regions for computing edges. Essentially, these local regions were selected based on their lower complexity and larger grey-scale values for the computation of illumination variation. Subsequently, histogram equalisation for enhanced feature combination by adding edge information for face recognition has been incorporated. The authors have used the CMU PIE and extended Yale B datasets for experimental validations. Lee et al. (2012) used the oriented local histogram equalisation technique to enhance images. It has been observed that edge orientation has served as a crucial feature for improving the recognition rate in extreme lighting conditions. Fu et al. (2015) have proposed an approach based on the simultaneous estimation of reflectance and illumination. The priors of both illumination and reflectance have been formulated by applying a Maximum A Posteriori (MAP). With the aid of the effective estimation of illumination and reflectance, they solved the MAP problem by using the alternating direction method. An image enhancement method has been proposed by Huang et al. (2018) that utilises the framelet regularisation technique to estimate reflectance. This method simultaneously calculates illumination and reflectance, preserving image details.

Despite illumination variation being a potential issue in different SSPP FR applications, fewer investigations have been proposed to handle the problem where lighting conditions cause degradation to the images (Liu et al., 2022; Xue & Ren, 2021). In addition, the lack of an image enhancement approach is the basic reason for not retrieving acceptable performance in such variations. The existing studies show that most proposed work for SSPP FR emphasises the feature extraction phase or classification phase, while ignoring pre-processing approaches that can enhance facial image quality (Fei et al., 2024; Ye et al., 2021). In PICS-DL, the proposed technique does not rely on any training mechanisms and instead exploits pertinent information contained in the face images. We emphasise illumination variations by complementing the Probabilistic Image Enhancement method (PIE) (Fu et al., 2015) with a DL Model. Hence, the presented study aims to develop an effective pre-processing approach for single-sample per-person face recognition in unconstrained environments.

THE PROPOSED FRAMEWORK

Overview of the Proposed Framework

The application of image enhancement to address illumination issues is well-documented in the literature (Anbarjafari et al., 2015; Fu et al., 2015; Huang et al., 2018; Mohd Sharif et al., 2024; Zhang et al., 2018; Zhuang et al., 2021). To mitigate illumination issues, these studies have proposed various methods, such as histogram equalisation, colour correction, and the Retinex method, for different images. The Retinex theory (Land, 1983; Land & McCann, 1971) posits that the human visual system

can handle illumination with non-constant brightness and colour. For SSPP face recognition, issues related to lighting and shading that are commonly associated with illumination problems can be resolved using Retinex-based methods. Given a probe face image, the possible illumination effect is detected and analysed first (Lee et al., 2012; Nikan & Hassanpour, 2020; Peng et al., 2019; Yi et al., 2015). The training phase of the proposed framework, which occurs before applying any image enhancement technique, is illustrated in Figure 1. In this phase, we utilised a pre-trained model, specifically FaceNet, to extract the face embeddings. Then, the classical Support Vector Machines (SVM) is used to train the classification model.

Figure 1

Training Phase of the Proposed PICS-DL Framework

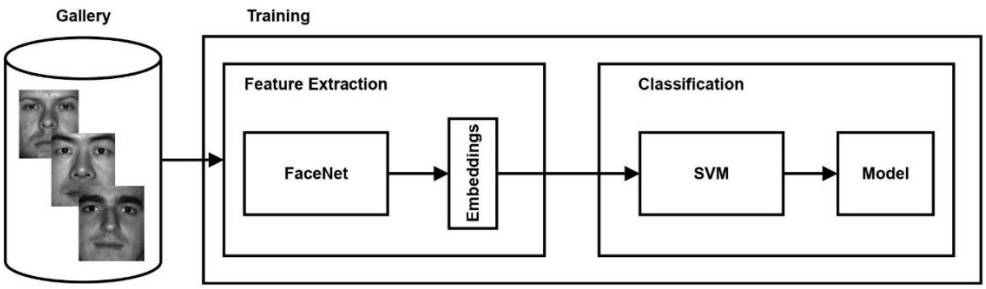

The testing phase of the proposed framework is shown in Figure 2. In this phase, the probe image is corrected using the PIE technique, which is based on the Retinex theory. The classical Retinex model describes the probe image as $S = I \cdot R$, where S represents the enhanced image, I and R correspond to the illumination and reflectance components, respectively. The component-based product operation is denoted by the dot operator. The well-known Bayesian approach is used to enhance the I and R components simultaneously as a posterior distribution. The optimisation algorithm is utilised to jointly estimate the I and R components in an efficient manner. This leads to reformulating the Maximum a Posteriori (MAP) estimation as an energy minimisation problem. To obtain a local optimal solution, the "Alternating Direction Method of Multipliers" (ADMM) approach (Goldstein & Osher, 2009) is employed.

The next step is to apply a Gamma correction technique to adjust the enhanced illumination (Fu et al., 2015; Kimmel et al., 2003; Li et al., 2018; Ng & Wang, 2011; Zhuang et al., 2021). Finally, an enhanced image is generated and used for face recognition. The face recognition process involves generating facial embeddings through a pre-trained FaceNet model, followed by label prediction against gallery images using an SVM classifier. SVM is one of the most prominent classification algorithms in supervised learning (Dougherty, 2012). It is a linear method that aims to maximise the margin and the perpendicular distance for support vectors, where the perpendicular distance measure is used to identify similarities between different support vectors. Hyperplanes are considered decision boundaries for classifying data. A decision line is created that separates N-dimensional space into classes to add a new data point. Compared to other supervised learners, SVM is used to find the hyperplane in an N-dimensional space to optimally classify the data points. Hence, it helps to classify high-dimensional data computationally effectively in comparison to other classifiers, such as kNN, which is a lazy learner for new data points. Furthermore, the SVM classifier exhibits generalizability even in small sample sizes, compared to DCNN or DL Models that require a large sample size for training.

Figure 2

Testing Phase with PIE of the PICS-DL Framework

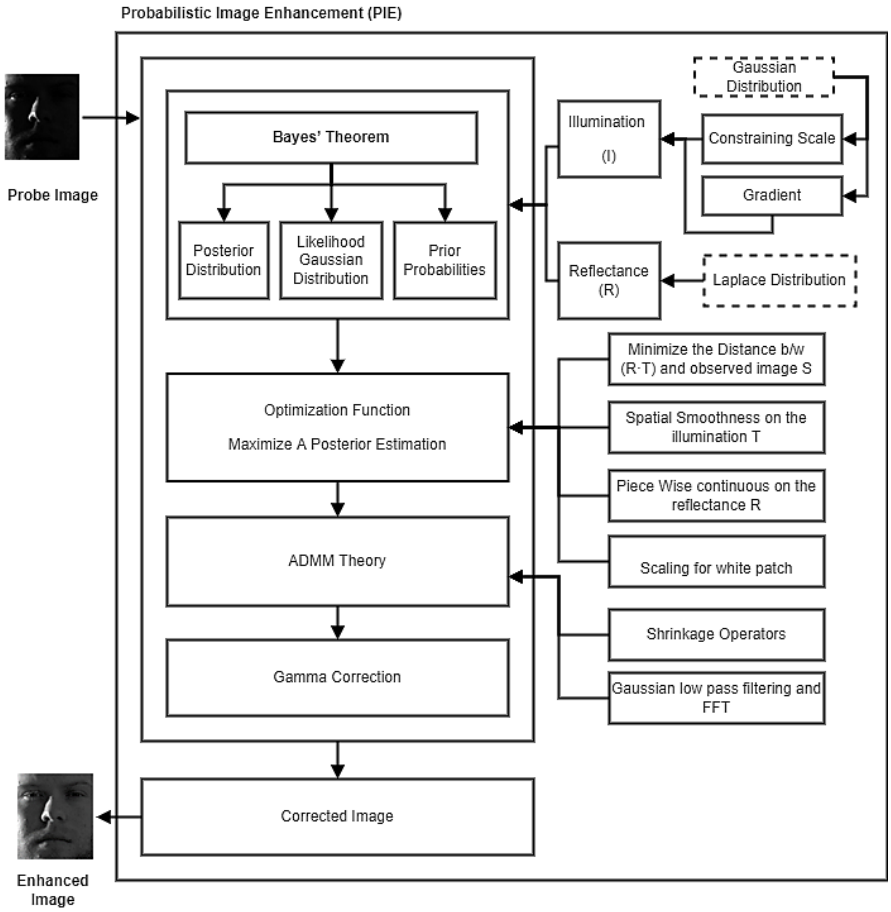

The following subsection will provide a detailed explanation of the adopted PIE method for image enhancement and the procedures relevant to feature embedding for recognition and classification.

The Proposed Probabilistic Image Enhancement Method

In SSPP, the presence of light and shade, occlusion, view variance, and so on affect recognition performance. In the proposed study, we attempt to resolve the illumination problem. Based on the Retinex theory, we denote the illumination with I and reflectance with R, for an observed image S. Equation 1 applies Bayes' theorem to estimate both illumination I and reflectance R from an observed image S:

$$p(I, R|S) \propto p(S|I, R)\, p(I)\, p(R) \quad (1)$$

where the posterior distribution is determined by $p(I, R|S)$ and the likelihood by $p(S|I, R)$. The prior probabilities are represented by $p(I)$ and $p(R)$ with respect to the illumination and reflectance.

Equation 2 computes the likelihood p(S|I, R) where N represents the normal distribution, ϵ represents the estimated error ($\epsilon = S - R \cdot I$) measured as an independent variable along with a Gaussian distribution having variance V_1 and zero mean, and the diagonal identity matrix represented by 1.

$$p(S, I|R) = N(\epsilon|S, V_1 1) \quad (2)$$

To compute the prior distribution p(R), multi-order gradient priors are introduced. These gradients are used for fine scaling and to complete the structures from probe images. For the intermediary results, the sample image is presented from the Extended Yale-B dataset. Figure 3 (a–d) shows a typical probe image and associated reflectance, illumination and v-channel outputs of the probe image. Further, the first-order, second-order image gradients and the Gaussian blur are shown in (e-g). The histogram distributions (bottom row, Figure 3) of these images clearly show a difference between the multi-order gradients of the reflectance and the illuminated images.

Figure 3

Phases of PIE (Extended Yale-B dataset) - (a) Original Image (b) Reflectance (c) Illumination (d) V-Channel (e) Horizontal gradient (f) Vertical gradient (g) Gaussian blur

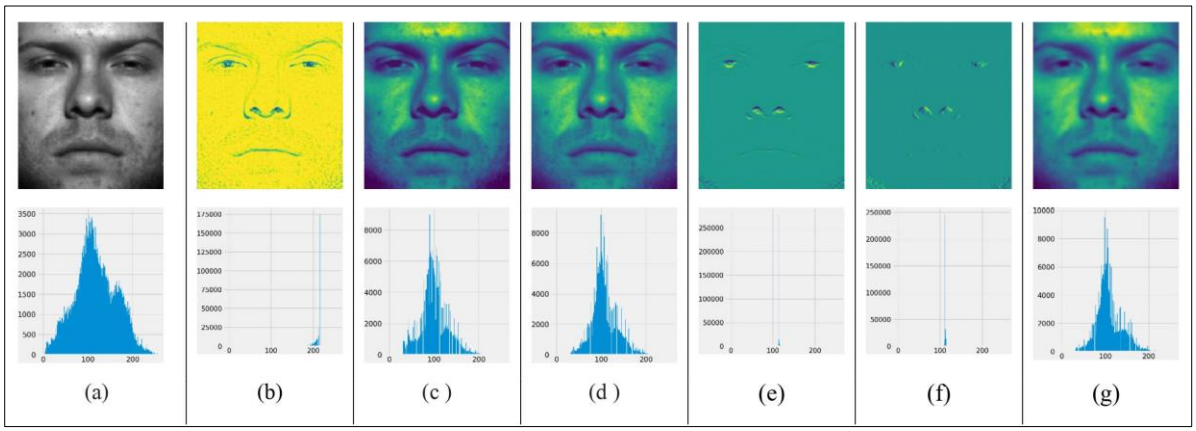

The reflectance images have more noise when compared to illuminated images, contain edges, and is piece-wise continuous (Fu et al., 2015; Fu et al., 2014; Ng & Wang, 2011; Wang et al., 2014; Yue et al., 2017; Zhuang et al., 2021). For this reason, the formulation of the distribution of gradients of reflectance is performed with a scale of s and a location of zero. In addition, two kinds of gradient distribution are considered, the first-order and second-order. The first-order gradient distribution follows a Laplacian model with location-zero and scale parameter s_1: $p_1(R) = L(\nabla R|0, s_1 1)$. A second-order gradient prior is applied to capture finer-scale edge features and mitigate staircase artefacts. This distribution is similarly modelled as a location-zero Laplacian with scale s_2: $p_2(R) = L(\nabla R|0, s_2 1)$. Here ∇ denotes the spatial gradient operator in both horizontal and vertical directions. The second-order derivative employs a discrete Laplacian kernel as $\nabla = [0, 1, 0; 1, -4, 1; 0, 1, 0]$. The combined prior p(R) integrates these components as specified in Equation 3.

$$p(R) = p_1(R)p_2(R) \quad (3)$$

The prior p(I) is modelled using two components. The first component assumes that the illumination is spatially smooth based on the distribution of gradients (Kimmel et al., 2003; Ng & Wang, 2011; Wang et al., 2014). Since the reflectance and illumination are not in the same numerical range, the second component is based on regularising and constraining the scale of illumination. The first component, i.e., $p_1(I) = N(\nabla I|0, V_3 1)$, is modelled using the gradients of a Gaussian distribution with variance V3 and zero mean, thereby enforcing smoothness in the spatial information of the illumination. Whereas, in the second component of the prior, the problem of scaling which is based on the white patch assumption is prevented by using the Gaussian distribution, i.e., $p_2(I) = N(I|I_0, V_4 1)$ having V_4 as a variance and I_0 is the mean of the Gaussian distribution. In this paper, the observed image S is averaged to estimate I_0, as the illumination does not exhibit an abrupt change. At the end, the prior p(I) is written as shown in Equation 4.

$$p(I) = p_1(I)p_2(I) \tag{4}$$

PIE-based Numerical Solution for the Probe Images

Representing $S = I \cdot R$ into the logarithmic domain, we have $log(S) = log(R) + log(I)$. According to the variational models and limitations in using the logarithmic domain, the linear model is adopted as explained by Fu et al. (2015). $E(I, R) = -log(p(I, R|S))$ is used to transform the MAP problem into an energy optimisation problem in order to estimate the illumination and reflectance. All the likelihoods and priors are used to model an optimisation problem as shown in Equation 5.

$$E(I, R) = ||(R.I) - S||_2^2 + \alpha\, ||\nabla I||_2^2 + \beta\, ||\nabla R||_1 + \gamma\, ||I - I_0||_2^2 \qquad \text{s.t.} \quad S < I \tag{5}$$

where positive parameters are α, β, γ and ‖‖p is the p-norm operator. In addition, since the value of R is in the range of 0 and 1, the function is subject to the constraint: S ≤ I. In order to minimize *E(I, R)*, the first span, i.e. $||(R.I) - S||_2^2$ which links to L_2 data fidelity, is used to minimise the distance between the observed image S and estimated (R·I). The second span, i.e. $||\nabla I||_2^2$ is used to apply the spatial smoothness to the illumination I. For the third span, i.e. $||\nabla R||_1$ implements the piece-wise continuous function on the reflectance R. The last span, i.e. $||I - I_0||_2^2$ is used to handle the scaling for the assumption of white patch and is based on L_2. Since the Gradient descent is not applicable for the optimisation of Equation 5 due to two unknown variables, R and I, optimisation is performed by the Alternating Direction Method of Multipliers (ADMM) (Goldstein & Osher, 2009). As a solution, an error term b and an auxiliary variable d are introduced, and subsequently, Equation 6 is rewritten as:

$$E(I.R, d, b) = ||(R.I) - S||_2^2 + \alpha\, ||\nabla I||_2^2 + \beta\{(\|d\|_1 + \lambda\, ||\nabla R - d + b||_2^2)\} + \gamma\, ||I - I0||_2^2 \qquad \text{s.t.} \quad S \leq I \tag{6}$$

According to ADMM theory, this optimisation function has minima and maxima and is divided into three sub-problems, which are solved. The parameter update for the j[th] iteration is as follows:

$$\begin{aligned}
&\text{(P1)}\ \ d^j = argmin_d\ ||d||_1 + \lambda\, ||\nabla R^{j-1} - d + b^{j-1}||_2^2 \\
&\text{(P2)}\ \ R^j = argmin_R\ ||R - \tfrac{S}{I^{j-1}})||_2^2 + \beta\, \lambda\, ||\nabla R - d^j + b^{j-1}||_2^2, \\
&\quad\ b^j = b^{j-1} + \nabla R^{j-1} - d \\
&\text{(P3)}\ \ I^j = argmin_I\ ||I - \tfrac{S}{R^j}||_2^2 + \alpha\, ||\nabla I||_2^2 + \gamma\, ||I - I_0||_2^2
\end{aligned} \tag{7}$$

In (P2) and (P3) $||R.I^{j-1} - S||_2^2$ is transformed into $||R - \frac{S}{I^{j-1}}||_2^2$ for calculation simplicity. The subproblems P1, P2, and P3 are considered as a closed form of the global optimal solution. For the update of b^j, the ADMM algorithm is explained below:

1. Algorithm for P1: In P1, the initialization of b^0 and $R^0 = 0$, in order to update the d^j at the j^{th} iteration, a shrinkage operation has been adopted:

$$d_h^j = shrink\left(\nabla_h R^{j-1} + b_h^{j-1}, \frac{1}{2\lambda}\right),$$
$$d_v^j = shrink\left(\nabla_v R^{j-1} + b_v^{j-1}, \frac{1}{2\lambda}\right), \quad (8)$$

where shrink $(x, \lambda) = \frac{x}{|x|}$ * max $(|x| - \lambda, 0)$ with $\frac{x}{|x|}$ equal to 0 when $|x| = 0$. h and v are the horizontal and vertical directions, respectively.

2. Algorithm for P2: I_0 is initialised through a method that is similar to centre-surround Retinex methods (Jobson et al., 1997a, 1997b; Rahman et al., 2004), which is known as the Gaussian low-pass filtering that is applied to the observed image. R^j has a closed-form solution as P2 is a least squares problem. In order to accelerate the process, the Fast Fourier Transformation (FFT) is used which is similar to many other studies (Goldstein & Osher, 2009; Ng & Wang, 2011). Equation 9 shows the updated R^j after setting the first-order derivative to zero in the frequency domain:

$$R^j = F^{-1}\left(\frac{F\left(\frac{S}{Ij^{-1}+\Delta}\right)+\beta\lambda\Phi}{F(1)+\beta\lambda\left(F*(\nabla_h)+F(\nabla_h)+F*(\nabla_v).F(\nabla_v)\right)}\right) \quad (9)$$

where $\Phi = F*(\nabla_h).F\left(d_h^j - b_h^{j-1}\right) + F*(\nabla_v).F\left(d_v^j - b_v^{j-1}\right)$, where F* is the conjugate transpose, F is the FFT operator, F^{-1} is the inverse FFT operator and ∇ is a slight +ve value that is used to elude the whole value from being infinity. To avoid matrix inversion, after the FFT, the derivative operator is diagonalised. For this, element-wise calculations are performed. At the j^{th} iteration, b^j is updated in Equation 10:

$$b_h^j = b_h^j + \nabla_h R^j - d_h^j,$$
$$b_v^j = b_v^j + \nabla_v R^j - d_v^j \quad (10)$$

This operation is the same as used in total variation (TV) denoising (Osher et al., 2005), which involves "adding back the noise" where R, b, and d are updated until $\varepsilon R = (\|R^j - R^{j-1}\| / \| R^{j-1}\|) \leq \varepsilon_1$.

3. Algorithm for P3: Since P3 is a least squares problem updating I^j is like R^j (Fu et al., 2015) represented by Equation 11.

$$I^j = F^{-1}\left(\frac{F\left(\gamma I_0 + O/(R^j+\Delta)\right)}{F(1)+\gamma+\alpha(F*(\nabla_h).F(\nabla_h)+F*(\nabla_v).F(\nabla_v))}\right) \quad (11)$$

According to the prior: $S \leq I$, after updating I, a simple correction has been made like:

$I^j = \max(I^j, S)$. I is updated until $\varepsilon_1 = (\| I^j - I^{j-1} \| / \| I^{j-1} \|) \leq \varepsilon_2$.

After estimating the illumination and reflectance, the illumination effect is adjusted to enhance the probe images. Specifically for the case of the SSPP problem, the gallery image is used for the training set, and the pre-processing step is applied to the probe images. Algorithm 1 describes the PIE method, which we have adapted to correct the illumination effect in the probe images.

To avoid the over-enhanced factor of reflectance, a Gamma correction operator is used for post-processing, as previously done in various studies (Kimmel et al., 2003; Ng & Wang, 2011; Wang et al., 2014). Gamma correction is applied to the illumination I using a parameter γ, and can be mathematically expressed in Equation 12:

$$I' = W\left(\frac{I}{W}\right)^{\frac{1}{\gamma}} \tag{12}$$

where W is set to 255 and the empirical parameter γ is 2.2. Finally, the enhanced image (Se) is presented by Equation 13:

$$S_e = R \cdot I' \tag{13}$$

The empirical parameter values used in experiments are $\alpha = 1000$, $\beta = 0.01$, $\gamma = 0.1$ and for $\lambda = 10$. Stopping parameters $\epsilon 1$ and $\epsilon 2$ have been set to 0.1.

Algorithm 1. Outline of the PIE Algorithm

Input: Input Facial image S, parameters α, β, γ, and λ
Stopping parameters ϵ_1 and ϵ_2
Initialization : $I^0 \leftarrow$ Gaussian filtering of S, $R^0 = 0$, $b^0 = 0$,
$I^0 \leftarrow$ average of S, set j = 1.
At the j-th iteration:
Update d^j using (8)
Update R^j using (9)
Update b^j using (10)
Update I^j using (11)
Update I^j using max(I_j, S)
Stopping criteria: if $\epsilon_R \leq \epsilon_1$ and $\epsilon_1 \leq \epsilon_2$, stop iteration,
Otherwise j = j+1 and continue the iteration
Output: Illumination I, Reflectance R

Feature Extraction using DCNN

In this proposed study, we extracted face embeddings using the classical FaceNet model, a DCNN model proposed by Google researchers in 2015 for face recognition systems. It operates on a batch of input layers and convolutional layers, followed by L_2 normalisation to produce face embeddings (Schroff et al., 2015). Technically, the input image size of 160×160×3 gets transformed into a 128-dimensional face embedding vector. The model learns facial features as a mapping using convolutional

layers and calculates the Euclidean distance in space to measure face similarity with the triplet loss function. Thus, the extraction of embedded feature vectors is performed and subsequently used for face recognition and verification (Ming et al., 2017).

The model creates embeddings of 128 dimensions, is used to cluster faces, and describes a face's significant characteristics. In the next step, it finds the minimum L_2 distance between the training face and the target face embedding. This is the well-known Euclidean distance, which is similar to the word embedding (Schroff et al., 2015), the nearest distance between two points in an N-dimensional space. Therefore, the distances for similar images will be closer than those for non-similar images. The steps involved in feature extraction using the FaceNet model are shown in Figure 4. FaceNet employed a novel strategy for triplet selection using face embeddings. Considering the embeddings of the same face image are called positives, the embeddings of different faces (in our case, probe images) are considered as negatives. The face that needs to be analysed is called the anchor (in the present study, it is actually the gallery image).

Figure 4

Representation of the FaceNet Model

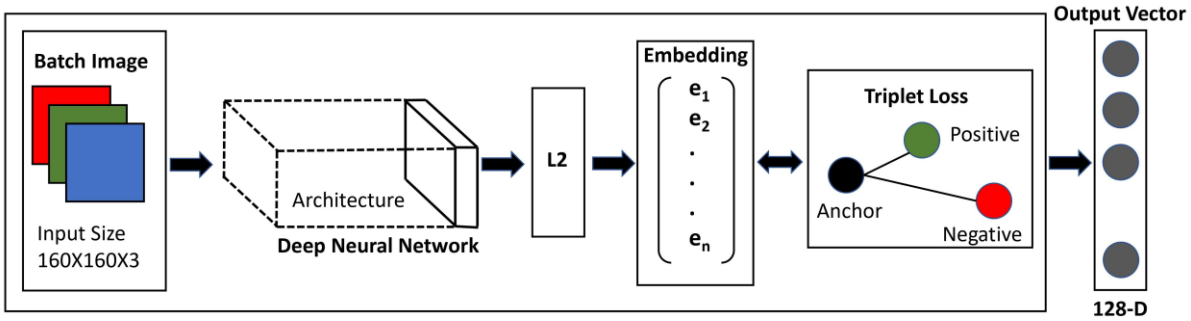

Hence, the loss is calculated for this triplet, i.e., positive, negative, and anchor, based on the Euclidean distance. FaceNet is trained to reduce the distance between an anchor image and positive samples of the same identity while increasing the distance between the anchor and negative samples from different identities. In this context, the goal is to guarantee that an anchor image x_j^a of a particular individual is positioned closer to all positive images x_i^p of the same individual than to any negative image x_i^n belonging to a different person, as illustrated in Equation 14.

$$||f(x_i^a) - f(x_i^p)||_2^2 + \alpha < ||f(x_i^a) - f(x_i^n)||_2^2 ,$$
$$\forall \left(f(x_i^a), f(x_i^p), f(x_i^n)\right) \epsilon \mathcal{T} \quad (14)$$

where α is denoted as a margin that is enforced between negative and positive pairs. All possible triplets of the training set are denoted by T, having N as a cardinality. The loss that is being minimised is calculated by Equation 15

$$\sum_i^N \left[\left|\left|f(x_i^a) - f(x_i^p)\right|\right|_2^2 - \left|\left|f(x_i^a) - f(x_i^n)\right|\right|_2^2 + \alpha\right]_+ \quad (15)$$

For the triplet selection and faster convergence, selection of triplets that violate the triplet constraint is important in Equation 14. By this, givenx_i^a, select an x_i^p (termed as hard positive) such that calculated in Equations 16 and 17:

$$Argmax_{x_i^p} \left|\left|f(x_i^a) - f(x_i^p)\right|\right|_2^2 \tag{16}$$

and similarity xi (termed as hard negative) such that:

$$Argmax_{x_i^n} \left|\left|f(x_i^a) - f(x_i^n)\right|\right|_2^2 \tag{17}$$

For the SSPP FR problem, we can relate the anchor image x_i^a to gallery image, positive image x_i^p to probe the image of the same person and the negative image x_i^n to probe the image of any other person. For the proposed approach, the weights of FaceNet are used as a transfer learner to extract the features.

EVALUATION AND RESULTS

Different experiments are conducted to evaluate the efficacy of the proposed solution introduced in this paper. The performance of the proposed model is evaluated with the existing Extended Yale-B dataset. The proposed approach aims to improve the overall quality of images affected by illumination effects. The proposed model aims to solve the problem of illumination in unconstrained conditions based on the following two criteria, which were considered while selecting the dataset: the selected datasets should have captured face images under a realistic environment of illumination problems in unconstrained conditions, and as part of the experimental procedure, all face images were normalised to a uniform dimension of 160×160 pixels with three color channels.

To compare the results of the proposed technique with those of existing ones, we have established different protocols for each experiment. In addition, for the comparison with the existing studies, we have selected five generic learning methods for comparison, viz., ESRC (Deng et al., 2012), SVDL (Yang et al., 2013), SSRC (Deng et al., 2013), CPL (Ji et al., 2017), and SGL (Pang et al., 2019). The comparative results of these studies were referred to in Pang et al. (2019). The results are also compared with those of IDGL (Pang et al., 2020) and RPRV (Xue & Ren, 2021). We compare our work with these studies because they use the same datasets and experimental setup as ours. Different experiments are conducted to analyse the performance of the proposed image enhancement technique for the illumination challenge for the SSPP FR problem. Table 1 presents the details of the images used in our experiments.

Table 1

Summary of Details of the Extended Yale-B Dataset used for the Evaluation

Database	No. of Subjects	No. of Samples	Color	(Actual Image size)
Extended Yale-B	20	1180	Gray	192 x 168
	30	1920		

Experiments on the Extended Yale-B Dataset

To perform the experiments with the Extended Yale-B dataset, we use five subsets in our experiments. These subsets contain face images that vary with different illumination settings by varying the angle between the light source direction and the camera axis. For the training set, subset 1 is selected which is under normal lighting conditions. Subsets 2 and 3 have images from slight to moderate luminance variations. Whereas subsets 4 and 5 have extreme lighting variations. Each subject has 64 images with varying illumination from 64 different directions. To compare the results of the proposed technique with those of existing techniques, we performed experiments with 20 and 30 subjects. Table 2 shows the number of images and angle variations. Subsets 2 to 5 are used for testing purposes. The test sample size is 57 images per subject for each experiment.

Table 2

Subsets of the Extended Yale-B Dataset According to Light Angle Source Direction

	Subset1	Subset2	Subset3	Subset4	Subset5
Illumination Angle	0^o-12^o	13^o-25^o	26^o-50^o	51^o-77^o	$>77^o$
No. of images per subject	7	12	12	14	19
Total Images (20 subjects)	140	240	240	280	380
Total Images (30 Subjects)	210	360	360	420	570

Figure 5

Extended Yale-B Face Image without Illumination Correction

Figure 6

Extended Yale-B Face Image with Illumination Correction

Figure 5 imparts the sample images of the first subject from each subset (i.e., Subset 1-5) without image enhancement, whereas Figure 6 shows the sample images of the first subject from each subset (i.e., Subset 2-5) with image enhancement of the proposed approach.

Experiments with Different Subjects

We have performed experiments with 20 and 30 subjects. Table 3 presents the results for different subjects and subsets, using various training images (T1 to T6) of subset 1 without image enhancement. The selection of 20 and 30 subjects was done by eliminating corrupted images as reported in (CVS, 2007; UCSD, 2005). For 20 subjects, it was observed that the results with subset 2 achieved 100% accuracy, whereas subset 3 achieved an average accuracy of 96%. For subset 4, the accuracy received is 81%, whereas for subset 5, the accuracy declined to 45%. For the case of 30 subjects, the results indicate that Subsets 2 and 3 achieve very high accuracy, even without applying any illumination corrections, because the illumination effect is too small. For the case of 30 subjects, subset 5 shows a decline in accuracy as compared to the other sets.

Table 3

Without PIE, with 20 and 30 Subjects

Subsets	Subjects	T1	T2	T3	T4	T5	T6	Average
Subset 2	20	100.00	100.00	100.00	100.00	100.00	100.00	100.00
	30	100.00	100.00	100.00	100.00	100.00	100.00	100.00
Subset 3	20	95.80	95.38	97.90	95.79	95.80	99.16	96.64
	30	96.09	95.53	96.65	95.25	95.25	97.77	96.09
Subset 4	20	81.99	80.15	80.52	83.82	80.88	81.25	81.43
	30	78.16	78.16	79.13	79.85	78.64	78.40	78.72
Subset 5	20	43.78	44.05	48.11	45.95	44.32	46.22	45.40
	30	42.86	44.11	44.82	45.18	44.29	43.75	44.17

Table 4 shows the results for 20 and 30 subjects when our proposed PIE method is applied. For the 20 subjects, the results indicate that there is no or minimal difference after applying image correction to subsets 2 and 3, because the illumination effect is too small to be corrected. Subset 4 exhibits an improvement of almost 10% after illumination correction. Subset 5 shows a remarkable improvement of almost 50% after illumination correction. For 30 subjects, subset 2 received 100% accuracy, whereas subset 3 received 98% accuracy. For subsets 4 and 5, the average accuracies are 90% and 94%, respectively.

Table 4

With PIE (20 and 30 Subjects)

Subsets	Subjects	T1	T2	T3	T4	T5	T6	Average
Subset 2	20	100.00	100.00	100.00	100.00	100.00	100.00	100.00
	30	100.00	100.00	100.00	100.00	100.00	100.00	100.00
Subset 3	20	97.90	97.06	98.74	98.32	98.32	99.58	98.32
	30	97.21	97.21	98.32	98.32	98.05	99.16	98.05
Subset 4	20	91.91	91.91	90.81	92.28	91.18	90.81	91.48
	30	90.53	91.26	89.32	91.02	90.53	89.32	90.33
Subset 5	20	95.41	95.68	93.51	94.32	95.14	95.14	94.86
	30	94.46	95.54	93.21	94.29	94.46	94.11	94.35

Comparison with and without PIE for All Subjects

The graphical comparison of face recognition accuracy is presented in Figures 7 and 8. The lower curve illustrates the degradation of performance under increasingly extreme illumination conditions for subsets 2-5 of the Extended Yale B dataset (Georghiades et al., 2001). Example images are presented on the horizontal axis with different illuminations. The upper curve indicates that our pre-processing approach significantly improves performance under challenging illumination conditions. Table 5 presents a comparative analysis of the proposed method's performance with and without PIE across subsets (2-5) and subjects (20 and 30). The results show that for both subject settings, the inclusion of PIE significantly improves recognition accuracy, especially in more challenging subsets. For 20 subjects, Subset 2 achieves a perfect accuracy of 100.00% with or without PIE, because the illumination effect is too small due to a well-illuminated image. Subset 3 shows a minor improvement, with an almost 1% increase after illumination correction. Subset 4 exhibits a substantial gain, with accuracy improving by nearly 10% after illumination correction. Subset 5 shows a remarkable improvement of almost 50% after illumination correction. The overall average accuracy for this setting increases by 15.30%, demonstrating the effectiveness of PICS-DL.

Figure 7

Comparison with and without PIE for 20 Subjects

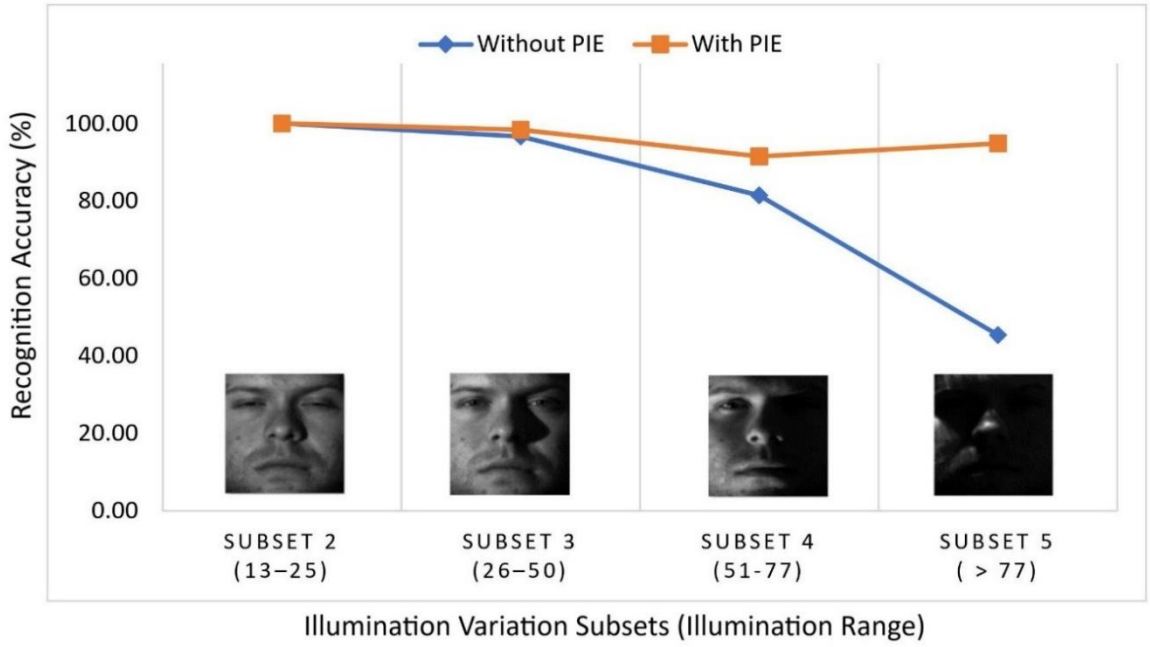

Figure 8

Comparison with and without PIE for 30 Subjects

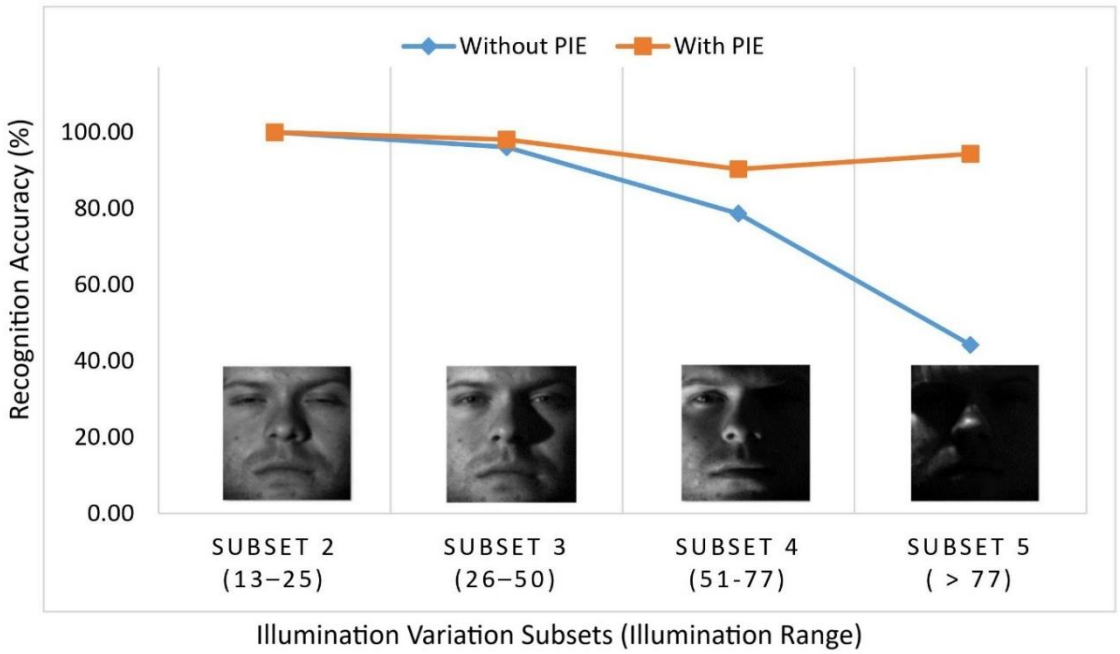

For the 30 subjects, the results indicate an overall improvement of 15.94% when comparing the results before and after applying the PIE. For subset 5, this improvement is nearly 50%, while for subset 2, no difference was observed. The average result also proves the effectiveness of PICS-DL (approximately 16% improvement in the overall results).

Table 5

PIE with 20 and 30 Subjects

Subjects	Subsets	Without PIE	With PIE	Improvement
20	Subset 2 (13-25)	100.00	100.00	0↔
	Subset 3 (26-50)	96.64	98.32	1.68↑
	Subset 4 (51-77)	81.43	91.48	10.05↑
	Subset 5 (> 77)	45.41	94.86	49.46↑
	Average	80.87	96.17	15.30↑
30	Subset 2 (13-25)	100.00	100.00	0↔
	Subset 3 (26-50)	96.09	98.05	1.96↑
	Subset 4 (51-77)	78.72	90.33	11.61↑
	Subset 5 (> 77)	44.17	94.35	50.18↑
	Average	79.74	95.68	15.94↑

Table 6 presents a detailed comparison of the proposed method with several state-of-the-art face recognition approaches, evaluated on the SSPP task across four subsets (2-5). For the 20 subjects, it is noted that for subset 2, a 100% accuracy is obtained for the existing and presented study. For Subset 3, the studies SGL (Pang et al., 2019) and RPRV (Xue & Ren, 2021) offer better results as compared to the PICS-DL. However, they showed a significant decline in performance as the complexity of the subsets increased, as seen in Subset 5. Subsequent methods, such as SGL (Pang et al., 2019), IDGL (Pang et al., 2020), and RPRV (Xue & Ren, 2021), demonstrated high accuracy across more challenging subsets, achieving average accuracies of 75.59%, 77.50%, and 76.92%, respectively.

The proposed method outperforms all existing approaches by a significant margin. While it maintains perfect accuracy on Subset 2 and near-perfect results on Subset 3 (98.32%), it demonstrates remarkable performance on the more challenging subsets, achieving 91.48% on Subset 4 and 94.86% on Subset 5. It leads to the highest average accuracy of 96.16%, indicating superior robustness and effectiveness in handling variations typical of SSPP face recognition scenarios.

Table 6

Recognition Rate Comparison with State-of-the-Art Methods

Method	No. of Subjects	Accuracy				Average Accuracy
		Subset2	Subset3	Subset4	Subset5	
ESRC (Deng et al., 2012)	-	99.83	95.33	61.43	16.05	68.16
SSRC (Deng et al., 2013b)	-	100.00	97.30	69.30	18.90	71.40
SVDL (Yang et al., 2013)	-	100.00	98.60	71.10	20.80	72.60
CPL (Ji et al., 2017)	-	100.00	98.33	70.71	20.37	72.35
SGL (Pang et al., 2019)	20	100.00	100.00	78.89	24.74	75.59
IDGL (Pang et al., 2020)	20	100.00	99.20	79.60	31.00	77.50
RPRV (Xue & Ren, 2021)	20	100.00	100.00	79.50	28.17	76.92
PICS-DL	20	100.00	98.32	91.48	94.86	96.17

Table 7 presents a comparative summary of various state-of-the-art techniques, where the experimental setup was not divided into subsets and only the overall accuracy was reported. Liu et al. (2022) introduced the CAE-BSJR method, which achieved an overall accuracy of 96.00% using 63 test samples per subject on a dataset of 10 subjects. Wang et al. (2019b) employed the HOG–LDB technique, attaining a high accuracy of 98.60% with 50 samples per subject across 20 subjects.

In another study, Liu, Yang, et al. (2019) proposed the MKCC-BOF approach, which achieved an accuracy of 93.60% using 30 subjects, although the number of test samples per subject was not specified. Similarly, Liu, Ding, et al. (2019) developed the LRGR-BSS method, which reached 95.50% accuracy using 63 samples per subject on 30 subjects. Ye et al. (2021) combined VGG with LESRC, but the approach performed relatively poorly, achieving only 66.40% accuracy with 63 test samples per subject on 30 subjects. Liu et al. (2021) introduced SOM-BC, yielding a slightly higher accuracy of 94.86% across 30 subjects; however, the number of test samples per subject was not specified. Finally, PICS-DL was also evaluated on a larger dataset comprising 30 subjects and 57 test samples per subject, achieving an accuracy of 95.68%. These results collectively demonstrate the varying effectiveness of SSPP face recognition methods under different experimental conditions.

Table 7

Recognition Rate Comparison with State-of-the-Art Methods

Researcher	Method	Test Samples Per Subject	Overall Accuracy	No. of Subjects
Liu et al. (2022)	CAE-BSJR	63	96.00	10
Wang et al. (2019)	HOG–LDB	50	98.60	20
PICS-DL (with 20 subjects)		57	96.17	20
Liu, Yang, et al. (2019)	MKCC-BOF	-	93.60	30
Liu, Ding, et al. (2019)	LRGR-BSS	63	95.50	30
Ye et al. (2021)	VGG+LESRC	63	66.40	30
Liu et al. (2021)	SOM-BC	-	94.86	30
PICS-DL (with 30 subjects)		57	95.68	30

By analysing the experimental results, we found that three major factors cause the most recognition errors in our experiment. Firstly, the image quality of the probe image is highly deteriorated, thereby making the enhancement quality of the image and the extracted features insufficient to accurately classify the probe face. Secondly, some probe images look similar, and the extracted features are not discriminative. It leads to erroneous predictions related to the enhanced quality of the face images. Finally, the last reason is the process of image capturing, which is why a few images do not contain a face. In our experiments, subsets 4 and 5 contain 6 and 8 corrupted face images, respectively.

CONCLUSION

We propose a method PICS-DL, to address the problem of SSPP FR under challenging illumination variations. The proposed approach addressed the problem by first analysing the illumination effects and then applying the probabilistic image enhancement technique to correct the illumination.

Comprehensive experiments have been conducted to correct illumination variations using the Extended Yale-B dataset for the SSPP FR. It has been demonstrated that the application of the PIE-based illumination correction pre-processing mechanism has substantially improved face recognition performance, comparable to state-of-the-art methods, especially when faces are subject to various illumination variations in uncontrolled conditions. Specifically, the face recognition accuracy achieved by the proposed PICS-DL has improved significantly by up to 16%. For future avenues, further enhancement may be possible by exploring methods that address illumination, coupled with occlusion, and pose variations.

REFERENCES

Abdelmaksoud, M., Nabil, E., Farag, I., & Hameed, H. A. (2020). A novel neural network method for face recognition with a single sample per person. *IEEE Access*, *8*, 102212-102221. https://doi.org/10.1109/ACCESS.2020.2999030

Adjabi, I., Ouahabi, A., Benzaoui, A., & Jacques, S. (2021). Multi-block color-binarized statistical images for single-sample face recognition. *Sensors*, *21*(3), 728. https://doi.org/10.3390/s21030728

Anbarjafari, G., Jafari, A., Jahromi, M. N. S., Ozcinar, C., & Demirel, H. (2015). Image illumination enhancement with an objective no-reference measure of illumination assessment based on Gaussian distribution mapping. *Engineering Science and Technology, An International Journal*, *18*(4), 696-703. https://doi.org/10.1016/j.jestch.2015.04.011

Arigbabu, O. A., Syed Ahmad, S. M., Wan Adnan, W. A., Yussof, S., & Mahmood, S. (2015). Soft biometrics: Gender recognition from unconstrained face images using local feature descriptor. *Journal of Information and Communication Technology (JICT)*, *14*, 111-122. https://e-journal.uum.edu.my/index.php/jict/article/view/8159

Azmeen, J., & Borah, D. J. (2021). Face recognition techniques, challenges: A review. *Soft Computing for Intelligent Systems*, 369-374. https://doi.org/10.1007/978-981-16-1048-6_27

Bouchene, M. M. (2024). Bayesian optimization of histogram of oriented gradients (HOG) parameters for facial recognition. *The Journal of Supercomputing*, *80*(14), 20118-20149. https://doi.org/10.1007/s11227-024-06259-7

Cuculo, V., D'Amelio, A., Grossi, G., Lanzarotti, R., & Lin, J. (2019). Robust single-sample face recognition by sparsity-driven sub-dictionary learning using deep features. *Sensors*, *19*(1), 146. https://doi.org/10.3390/s19010146

CVS. (2007). Yale Face Database. http://cvc.cs.yale.edu/cvc/projects/yalefacesB/corrupt.html

Deng, W., Hu, J., & Guo, J. (2012). Extended SRC: Undersampled face recognition via intraclass variant dictionary. *IEEE Transactions on Pattern Analysis and Machine Intelligence*, *34*(9), 1864-1870. https://doi.org/10.1109/TPAMI.2012.30

Deng, W., Hu, J., & Guo, J. (2013). In defense of sparsity based face recognition. In *Proceedings of the IEEE Conference on Computer Vision and Pattern Recognition* (pp. 399-406). https://doi.org/10.1109/CVPR.2013.58

Dey, N. (2019). Uneven illumination correction of digital images: A survey of the state-of-the-art. *Optik*, *183*, 483-495. https://doi.org/10.1016/j.ijleo.2019.02.118

Dougherty, G. (2012). *Pattern recognition and classification: An introduction*. Springer Science & Business Media. https://doi.org/10.1007/978-1-4614-5323-9

Fei, R., Zhang, J., Bo, L., Zhang, H., Li, H., & Li, M. (2024). Joint multi-subspace feature learning with singular value decomposition for robust single-sample face recognition. *Computers and Electrical Engineering*, *114*, 109085. https://doi.org/10.1016/j.compeleceng.2024.109085

Filippidou, F. P., & Papakostas, G. A. (2020). Single sample face recognition using convolutional neural networks for automated attendance systems. In *2020 Fourth International Conference on Intelligent Computing in Data Sciences (ICDS)* (pp. 1-6). IEEE. https://doi.org/10.1109/ICDS50568.2020.9268759

Fu, X., Liao, Y., Zeng, D., Huang, Y., Zhang, X.-P., & Ding, X. (2015). A probabilistic method for image enhancement with simultaneous illumination and reflectance estimation. *IEEE Transactions on Image Processing*, *24*(12), 4965-4977. https://doi.org/10.1109/TIP.2015.2474701

Fu, X., Zhuang, P., Huang, Y., Liao, Y., Zhang, X. P., & Ding, X. (2014, October). A retinex-based enhancing approach for single underwater image. In *2014 IEEE International Conference on Image Processing (ICIP)* (pp. 4572-4576). IEEE. https://doi.org/10.1109/ICIP.2014.7025927

Gan, W., Yang, H., Zeng, J., & Chen, F. (2020). Auxiliary dictionary of diversity learning for face recognition with a single sample per person. *International Journal on Artificial Intelligence Tools*, *29*(05), 2050015. https://doi.org/10.1142/S0218213020500153

Georghiades, A. S., Belhumeur, P. N., & Kriegman, D. J. (2001). From few to many: Illumination cone models for face recognition under variable lighting and pose. *IEEE Transactions on Pattern Analysis and Machine Intelligence*, *23*(6), 643-660. https://doi.org/10.1109/34.927464

Goldstein, T., & Osher, S. (2009). The split Bregman method for L1-regularized problems. *SIAM Journal on Imaging Sciences*, *2*(2), 323-343. https://doi.org/10.1137/080725891

Huang, Y.-S., & Alhlffee, M. H. B. (2023). Improving face recognition by integrating decision forest into GAN. *Applied Artificial Intelligence*, *37*(1), 2175108. https://doi.org/10.1080/08839514.2023.2175108

Huang, Z., Huang, L., Li, Q., Zhang, T., & Sang, N. (2018). Framelet regularization for uneven intensity correction of color images with illumination and reflectance estimation. *Neurocomputing*, *314*, 154-168. https://doi.org/10.1016/j.neucom.2018.06.063

Ji, H.-K., Sun, Q.-S., Ji, Z.-X., Yuan, Y.-H., & Zhang, G.-Q. (2017). Collaborative probabilistic labels for face recognition from single sample per person. *Pattern Recognition*, *62*, 125-134. https://doi.org/10.1016/j.patcog.2016.08.007

Jobson, D. J., Rahman, Z.-U., & Woodell, G. A. (1997a). A multiscale retinex for bridging the gap between color images and the human observation of scenes. *IEEE Transactions on Image Processing*, *6*(7), 965-976. https://doi.org/10.1109/83.597272

Jobson, D. J., Rahman, Z.-U., & Woodell, G. A. (1997b). Properties and performance of a center/surround retinex. *IEEE Transactions on Image Processing*, *6*(3), 451-462.

Kimmel, R., Elad, M., Shaked, D., Keshet, R., & Sobel, I. (2003). A variational framework for retinex. *International Journal of Computer Vision*, *52*(1), 7-23. https://doi.org/10.1109/83.557356

Land, E. H. (1983). Recent advances in retinex theory and some implications for cortical computations: color vision and the natural image. *Proceedings of the National Academy of Sciences of the United States of America*, *80*(16), 5163. https://doi.org/10.1073/pnas.80.16.5163

Land, E. H., & McCann, J. J. (1971). Lightness and retinex theory. *Journal of the Optical Society of America*, *61*(1), 1-11. https://doi.org/10.1364/JOSA.61.000001

Lee, P.-H., Wu, S.-W., & Hung, Y.-P. (2012). Illumination compensation using oriented local histogram equalization and its application to face recognition. *IEEE Transactions on Image Processing*, *21*(9), 4280-4289. https://doi.org/10.1109/TIP.2012.2202670

Li, M., Liu, J., Yang, W., Sun, X., & Guo, Z. (2018). Structure-revealing low-light image enhancement via robust retinex model. *IEEE Transactions on Image Processing*, *27*(6), 2828-2841. https://doi.org/10.1109/TIP.2018.2810539

Liu, F., Ding, Y., Xu, F., & Ye, Q. (2019). Learning low-rank regularized generic representation with block-sparse structure for single sample face recognition. *IEEE Access*, *7*, 30573-30587. https://doi.org/10.1109/ACCESS.2019.2903333

Liu, F., Tang, J., Song, Y., Zhang, L., & Tang, Z. (2015). Local structure-based sparse representation for face recognition. *ACM Transactions on Intelligent Systems and Technology (TIST)*, *7*(1), 1-20. https://doi.org/10.1145/2733383

Liu, F., Wang, F., Ding, Y., & Yang, S. (2021). SOM-based binary coding for single sample face recognition. *Journal of Ambient Intelligence and Humanized Computing*, 1-11. https://doi.org/10.1007/s12652-021-03255-0

Liu, F., Wang, F., Wang, Y., Zhou, J., & Xu, F. (2022). Cycle-autoencoder based block-sparse joint representation for single sample face recognition. *Computers and Electrical Engineering*, *101*, 108003. https://doi.org/10.1016/j.compeleceng.2022.108003

Liu, F., Yang, S., Ding, Y., & Xu, F. (2019). Single sample face recognition via BoF using multistage KNN collaborative coding. *Multimedia Tools and Applications*, *78*(10), 13297-13311. https://doi.org/10.1007/s11042-018-7002-5

Mehdipour Ghazi, M., & Kemal Ekenel, H. (2016). A comprehensive analysis of deep learning based representation for face recognition. In *Proceedings of the IEEE Conference on Computer Vision and Pattern Recognition Workshops* (pp. 34-41). https://doi.org/10.1109/CVPRW.2016.20

Ming, Z., Chazalon, J., Luqman, M. M., Visani, M., & Burie, J. C. (2017, October). Simple triplet loss based on intra/inter-class metric learning for face verification. In *2017 IEEE International Conference on Computer Vision Workshops (ICCVW)* (pp. 1656-1664). IEEE. https://doi.org/10.1109/ICCVW.2017.194

Mohd Sharif, N. A., Harun, N. H., & Yusof, Y. (2024). Colour image enhancement model of retinal fundus image for diabetic retinopathy recognition. *Journal of Information and Communication Technology (JICT)*, *23*(2), 293-334. https://doi.org/10.32890/jict2024.23.2.5

Mokhayeri, F., & Granger, E. (2020). A paired sparse representation model for robust face recognition from a single sample. *Pattern Recognition*, *100*, 107129. https://doi.org/10.1016/j.patcog.2019.107129

Mokhayeri, F., Granger, E., & Bilodeau, G.-A. (2018). Domain-specific face synthesis for video face recognition from a single sample per person. *IEEE Transactions on Information Forensics and Security*, *14*(3), 757-772. https://doi.org/10.1109/TIFS.2018.2866295

Ng, M. K., & Wang, W. (2011). A total variation model for Retinex. *SIAM Journal on Imaging Sciences*, *4*(1), 345-365. https://doi.org/10.1137/100806588

Nikan, F., & Hassanpour, H. (2020). Face recognition using non-negative matrix factorization with a single sample per person in a large database. *Multimedia Tools and Applications*, *79*(37), 28265-28276. https://doi.org/10.1007/s11042-020-09394-4

Oloyede, M. O., Hancke, G. P., & Myburgh, H. C. (2020). A review on face recognition systems: Recent approaches and challenges. *Multimedia Tools and Applications*, *79*(37), 27891-27922. https://doi.org/10.1007/s11042-020-09261-2

Osher, S., Burger, M., Goldfarb, D., Xu, J., & Yin, W. (2005). An iterative regularization method for total variation-based image restoration. *Multiscale Modeling & Simulation*, *4*(2), 460-489. https://doi.org/10.1137/040605412

Pang, M., Cheung, Y.-M., Shi, Q., & Li, M. (2020). Iterative dynamic generic learning for face recognition from a contaminated single-sample per person. *IEEE Transactions on Neural Networks and Learning Systems*, *32*(4), 1560-1574. https://doi.org/10.1109/TNNLS.2020.2985099

Pang, M., Cheung, Y.-M., Wang, B., & Lou, J. (2019). Synergistic generic learning for face recognition from a contaminated single sample per person. *IEEE Transactions on Information Forensics and Security*, *15*, 195-209. https://doi.org/10.1109/TIFS.2019.2919950

Peng, Y., Shi, H., Wu, H., Li, R., Kwok, N., Liu, S. C., Liu, S., & Rahnam, M. A. (2019). An optimum shift-and-weighted brightness mapping for low-illumination image restoration. *The Imaging Science Journal*, *67*(4), 187-201. https://doi.org/10.1080/13682199.2019.1592891

Rahman, Z.-U., Jobson, D. J., & Woodell, G. A. (2004). Retinex processing for automatic image enhancement. *Journal of Electronic Imaging*, *13*(1), 100-110. https://doi.org/10.1117/1.1636183

Ríos-Sánchez, B., Costa-da-Silva, D., Martín-Yuste, N., & Sánchez-Ávila, C. (2019). Deep learning for facial recognition on single sample per person scenarios with varied capturing Conditions. *Applied Sciences*, *9*(24), 5474. https://doi.org/10.3390/app9245474

Schroff, F., Kalenichenko, D., & Philbin, J. (2015). Facenet: A unified embedding for face recognition and clustering. In *Proceedings of the IEEE Conference on Computer Vision and Pattern Recognition* (pp. 815-823). https://doi.org/10.1109/CVPR.2015.7298682

Silva, A., & Farias, R. (2025). AD-VAE: Adversarial disentangling variational autoencoder. *Sensors*, *25*(5), 1574. https://doi.org/10.3390/s25051574

Taigman, Y., Yang, M., Ranzato, M. A., & Wolf, L. (2014). Deepface: Closing the gap to human-level performance in face verification. In *Proceedings of the IEEE Conference on Computer Vision and Pattern Recognition* (pp. 1701-1708). https://doi.org/10.1109/CVPR.2014.220

Tran, Q. M., Pham, V. T., Nga, D. T. T., & The Bao, P. (2022). Evaluating the efficacy of small face recognition by convolutional neural networks with interpolation based on auto-adjusted parameters and transfer learning. *Applied Artificial Intelligence*, *36*(1), 2012982. https://doi.org/10.1080/08839514.2021.2012982

UCSD. (2005). http://cvc.cs.yale.edu/cvc/projects/yalefacesB/yalefacesB.html

Wang, H., Zhang, D., & Miao, Z. (2019). Face recognition with single sample per person using HOG–LDB and SVDL. *Signal, Image and Video Processing*, *13*(5), 985-992. https://doi.org/10.1007/s11760-019-01436-1

Wang, L., Xiao, L., Liu, H., & Wei, Z. (2014). Variational Bayesian method for retinex. *IEEE Transactions on Image Processing*, *23*(8), 3381-3396. https://doi.org/10.1109/TIP.2014.2324813

Wang, M., & Deng, W. (2021). Deep face recognition: A survey. *Neurocomputing*, *429*, 215-244. https://doi.org/10.1016/j.neucom.2020.10.08

Xue, S., & Ren, H. P. (2021). Single sample per person face recognition algorithm based on the robust prototype dictionary and robust variation dictionary construction. *IET Image Processing*, *16*(3), 742-754. https://doi.org/10.1049/ipr2.12381

Yang, M., Van Gool, L., & Zhang, L. (2013). Sparse variation dictionary learning for face recognition with a single training sample per person. In *Proceedings of the IEEE International Conference on Computer Vision* (pp. 689-696). https://doi.org/10.1109/ICCV.2013.91

Yang, M., Wen, W., Wang, X., Shen, L., & Gao, G. (2020). Adaptive convolution local and global learning for class-level joint representation of facial recognition with a single sample per data subject. *IEEE Transactions on Information Forensics and Security*, *15*, 2469-2484. https://doi.org/10.1109/TIFS.2020.2965301

Ye, M., Cheng, Y., Lan, X., & Zhu, H. (2019). Improving night-time pedestrian retrieval with distribution alignment and contextual distance. *IEEE Transactions on Industrial Informatics*, *16*(1), 615-624. https://doi.org/10.1109/TII.2019.2946030

Ye, M.-J., Hu, C.-H., Wan, L.-G., & Lei, G.-H. (2021). Fast single sample face recognition based on sparse representation classification. *Multimedia Tools and Applications*, *80*(3), 3251-3273. https://doi.org/10.1007/s11042-020-09855-w

Yi, J., Mao, X., Chen, L., Xue, Y., Rovetta, A., & Caleanu, C.-D. (2015). Illumination normalization of face image based on illuminant direction estimation and improved retinex. *PloS One*, *10*(4), e0122200. https://doi.org/10.1371/journal.pone.0122200

Yue, H., Yang, J., Sun, X., Wu, F., & Hou, C. (2017). Contrast enhancement based on intrinsic image decomposition. *IEEE Transactions on Image Processing*, *26*(8), 3981-3994. https://doi.org/10.1109/TIP.2017.2703078

Zeng, J., Zhao, X., Gan, J., Mai, C., Zhai, Y., & Wang, F. (2018). Deep convolutional neural network used in single sample per person face recognition. *Computational Intelligence and Neuroscience*, *2018*(1), 3803627. https://doi.org/10.1155/2018/3803627

Zeng, J., Zhao, X., Qin, C., & Lin, Z. (2017, December). Single sample per person face recognition based on deep convolutional neural network. In *2017 3rd IEEE International Conference on Computer and Communications (ICCC)* (pp. 1647-1651). IEEE. https://doi.org/10.1109/CompComm.2017.8322819

Zhang, Q., Yuan, G., Xiao, C., Zhu, L., & Zheng, W. S. (2018, October). High-quality exposure correction of underexposed photos. In *Proceedings of the 26th ACM International Conference on Multimedia* (pp. 582-590). https://doi.org/10.1145/3240508.3240595

Zhang, Y., Hu, C., & Lu, X. (2019). IL-GAN: Illumination-invariant representation learning for single sample face recognition. *Journal of Visual Communication and Image Representation*, *59*, 501-513. https://doi.org/10.1016/j.jvcir.2019.02.007

Zhang, Z., Zhang, L., & Zhang, M. (2021). Dissimilarity-based nearest neighbor classifier for single-sample face recognition. *The Visual Computer*, *37*(4), 673-684. https://doi.org/10.1007/s00371-020-01827-3

Zhuang, P., Li, C., & Wu, J. (2021). Bayesian retinex underwater image enhancement. *Engineering Applications of Artificial Intelligence*, *101*, 104171. https://doi.org/10.1016/j.engappai.2021.104171